

1 **Title:**

2 Key structural features of Boreal forests may be detected directly using L-moments from
3 airborne lidar data

4

5 **Authors:**

6 Rubén Valbuena ^{*(1)}, Matti Maltamo⁽¹⁾, Lauri Mehtätalo ⁽²⁾, Petteri Packalen ⁽¹⁾

7

8 **Affiliations:**

9 (1) University of Eastern Finland, School of Forest Sciences, PO Box 111. Joensuu,

10 Finland; rubenval@uef.fi; matti.maltamo@uef.fi; petteri.packalen@uef.fi

11 (2) University of Eastern Finland. School of Computing. PO Box 111. Joensuu, Finland;

12 lauri.mehtatalo@uef.fi

13 *Corresponding author.

14

15

16

17

18

19

20

21

22

23 **Abstract**

24 This article introduces a novel methodology for automated classification of forest areas from
25 airborne laser scanning (ALS) datasets based on two direct and simple rules: L-coefficient of
26 variation $Lcv = 0.5$ and L-skewness $Lskew = 0$, thresholds based on descriptors of the
27 mathematical properties of ALS height distributions. We observed that, while $Lcv > 0.5$ may
28 represent forests with large tree size inequality, $Lskew > 0$ can be an indicator for areas
29 lacking a closed dominant canopy. $Lcv = 0.5$ discriminated forests with trees of approximately
30 equal sizes (even tree size classes) from those with large tree size inequality (uneven tree size
31 classes) with kappa $\kappa = 0.48$ and overall accuracy $OA = 92.4\%$, while $Lskew = 0$ segregated
32 oligophotic and euphotic zones with $\kappa = 0.56$ and $OA = 84.6\%$. We showed that a supervised
33 classification could only marginally improve some of these accuracy results. The rule-based
34 approach presents a simple method for detecting structural properties key to tree competition
35 and potential for natural regeneration. The study was carried out with low-density datasets from
36 the national program on ALS surveying of Finland, which shows potential for replication with
37 the ALS datasets typically acquired at nation-wide scales. Since the presented method was
38 based on deductive mathematical rules for describing distributions, it stands out from inductive
39 supervised and unsupervised classification methods which are more commonly used in remote
40 sensing. Therefore, it presents an opportunity for deducing physical relations which could
41 partly eliminate the need for supporting ALS applications with field plot data for training and
42 modelling, at least in Boreal forest ecosystems.

43 **Key words**

44 Airborne laser scanning; L-moments; Gini Coefficient; L-coefficient of variation; forest
45 structure; tree size inequality; shade-tolerance.

46

47 **1. Introduction**

48 Airborne laser scanning (ALS) can be a valuable tool for studying structural properties of
49 forests (Lefsky et al., 1999a; Drake et al., 2002; Frazer et al., 2005; Maltamo et al., 2005;
50 Valbuena et al., 2016a). The relationships of ALS to forest structure can be employed to analyse
51 asymmetric competition among trees (Kellner & Asner, 2009), and hence forest growth
52 conditions (Stark et al., 2010). In fully-stocked forests (Gove, 2004) light resource pre-emption
53 drives asymmetric competition processes, leading to mortality of the least competitive trees
54 (Weiner, 1990). These are forests with closed canopies and structural properties yielding shady
55 areas, i.e. oligophotic zones (sensu Lefsky et al., 2002), under the dominant tree crowns. In
56 turn, detecting forest areas with light resource availability, which are characterized by large
57 euphotic zones (sensu Lefsky et al., 2002), can be key to monitoring forest disturbance and
58 regeneration. Several metrics derived from ALS height distributions have potential for
59 describing these key characteristics related to forest structure (Zimble et al., 2003). For this
60 reason, studies on ALS-based forest structure characterization by statistical inductive methods,
61 which relate ALS metrics to field attributes empirically, are commonplace (Hall et al., 2005;
62 Lefsky et al., 2005; Dalponte et al., 2008; Pascual et al., 2008; Disney et al., 2010; Jaskierniak
63 et al., 2011; Ozdemir & Donoghue, 2013; Valbuena et al., 2014).

64 Size hierarchy among trees growing in the vicinity influences competition processes in the
65 forest community (Weiner, 1990; Valbuena et al., 2012). Knox et al. (1989) suggested the Gini
66 coefficient (GC) (Gini, 1921) as a consistent descriptor of tree size inequality, and hence a
67 reliable indicator of competition conditions in the forest (Cordonnier & Kunstler, 2015). For
68 this reason, in the context of ALS estimation, the GC of tree sizes has been used as a basis for
69 stratifying the forest area into homogeneous structural types (Bollandsås & Næsset, 2007;
70 Valbuena et al., 2013a). Furthermore, Knox et al. (1989) also suggested the inclusion of

71 skewness as a complement to the *GC* in describing forest structural properties. For this reason,
72 Valbuena et al. (2013a) included asymmetry in their analysis of forest structural properties, to
73 study relations of relative dominance between different strata in the forest vertical profile.

74 While Bollandsås & Næsset (2007) employed stand register data from previous inventories for
75 carrying out their stratification, it would be advantageous if the same remote sensing material
76 could be used for wall-to-wall predictions of forest structure indicators and classifications into
77 forest structural types (Lefsky et al., 1999b; Drake et al., 2002). In particular, Ozdemir &
78 Donoghue (2013) and Valbuena et al. (2013b; 2016a) obtained predictions of the *GC* of tree
79 size inequality with reliable accuracy. As previous research has concentrated on the forest
80 response (Lefsky et al., 1999a; Valbuena et al., 2013a), and on its analysis and estimation by a
81 wide range of different statistical methods – such as analysis of variance (Zimble et al., 2003),
82 canonical correlation (Lefsky et al., 2005), parametric (Hall et al., 2005) and non-parametric
83 (Valbuena et al., 2014) modelling, histogram thresholding (Maltamo et al., 2005), or finite
84 mixtures (Jaskierniak et al., 2011) –, the next question to answer would be: do the ALS metrics
85 have, by themselves, capacity to discriminate among forest structural types, making no use of
86 statistical methods linking field data to ALS metrics?.

87 Moments are quantitative measurements of probability density distributions employed to
88 summarize their properties. The most conventional are the product moments, expected values
89 of the powers of a random variable which lead to the use of mean, variance and skewness as
90 measures for location, scale and shape. These descriptors of ALS return height distributions
91 are metrics commonly employed as auxiliary variables in forest assessment (e.g., Næsset, 2002;
92 White et al., 2013). Alternatively, Frazer et al. (2011) and Ozdemir & Donoghue (2013)
93 recently drew the attention towards the L-moments, a set of statistics known by their sample
94 efficiency (i.e., reliability at low sample sizes) and robustness to outliers, compared to

95 conventional moments (Hosking, 1990). Consider a sample order statistic $X_{k:r}$ – the k^{th}
 96 smallest observation in a sample of size r –, which is a many-to-one transformation of a random
 97 sample of size r , and therefore a random variable. The L-moments are based on its expected
 98 values $E(X_{k:r})$ (Appendix A). Moreover, L-moment ratios have the advantage of being
 99 bounded by finite intervals (Hosking 1989), making them comparable among ALS
 100 distributions differing in their mean height. The L-coefficient of variation (Lcv) and the L-
 101 skewness ($Lskew$) are two types of L-moment ratios (Appendix A.2). Lcv is the ratio of the
 102 second ($L2$) to the first ($L1$) L-moments:

103 (1)
$$Lcv = \frac{L2}{L1} = \frac{E(X_{2:2}) - E(X_{1:2})}{2E(X)},$$

104 where $E(X)$ is the expected value of X . In the case of ALS metrics, the variable X is the height
 105 of ALS returns. The Lcv is mathematically equivalent to the GC (Appendix A.3), and therefore
 106 the same properties apply to both of them. For instance, they are scale-invariant, and for
 107 positive random variables their values are bounded within the $[0, 1]$ interval (Hosking, 1989).
 108 Also, Valbuena et al. (2012) showed that an asymptote at $GC = 0.5$ represents the case of
 109 maximum entropy among tree sizes in the forest. On the other hand, $Lskew$ is the ratio of the
 110 third ($L3$) to the second ($L2$) L-moments:

111 (2)
$$Lskew = \frac{L3}{L2} = \frac{E(X_{3:3}) - 2E(X_{2:3}) + E(X_{1:3})}{E(X_{3:3}) - E(X_{1:3})}.$$

112 In the case of $Lskew$, its theoretical bounds are $[-1, 1]$ (Hosking, 1989). The value of $Lskew =$
 113 0 corresponds to a symmetric distribution, while positive or negative values denote the type of
 114 asymmetry for the distribution of ALS heights. This article employs these mathematical
 115 properties of L-moments for describing ALS height distributions, in contrast to inductively
 116 researching explanatory potential in relation to field data attributes.

117 The aim of this research was to develop simple methods for explaining key features related to
118 forest structure from few L-moment ratios of ALS returns. *Lcv* and *Lskew* were used for
119 detecting tree size inequality and light availability, and they were utilized for an automated
120 classification of forests from ALS datasets, which was applied directly without the use of field
121 data. The idea builds upon the hypothesis that two deductive mathematical rules, $Lcv = 0.5$
122 and $Lskew = 0$, may be used to classify the forest area into two groups, based solely on the
123 ALS height distributions. We studied whether such classifications would be sound in terms of
124 explaining properties of size inequality among trees growing in vicinity (even or uneven tree
125 sizes) and competitive conditions for light in the forest community (oligophotic or euphotic).
126 We compared the reliability of the rule-based method to results obtained from a supervised
127 classification. This article discusses suitable applications for this rule-based method.

128 **2. Materials**

129 *2.1. Study area and ALS data*

130 The research was conducted in a 252,000 ha study area including approximately 200,000 ha of
131 the Boreal forest ecosystems typically found in the region of North Karelia (Finland), which
132 consists of forests dominated by Scots pine (*Pinus sylvestris* L.) Norway spruce (*Picea abies*
133 (L.) Karst.) or Birch species (*Betula* spp.) with various degrees of admixtures also with other
134 deciduous trees (such as *Alnus* spp., *Populus* spp. etc). The ALS data were acquired by Blom
135 Kartta Oy (Finland) during May 2012 with an ALS60 system from Leica Geosystems
136 (Switzerland). A flying height of 2,300 m above ground rendered an average density of 0.91
137 pulses per squared-meter. Country-wide laser data are being consistently acquired using
138 broadly similar parameters (National Land Survey of Finland; NLS, 2013). Methods may
139 therefore be consistently replicated throughout the country, bringing potential for upscaling the
140 results obtained at national-level.

141 Heights above ground for individual ALS returns were calculated by subtracting the digital
142 terrain model provided by the NLS. We considered that, as seedlings and saplings were
143 included in field mensuration (Valbuena et al., 2016b), their influence in laser pulse
144 interception had to be accounted for in ALS metric computation. Consequently, just a very
145 small height threshold of 0.1 m was used, only with the intention to mask out the influence of
146 the ground. Sample estimates of L-moments and their ratios (Wang, 1996) were computed from
147 the heights of all the ALS returns located within each cell over a regular grid covering the entire
148 study area. The spatial resolution of this grid was $16\text{ m} \times 16\text{ m}$, a customary practice in Finland
149 that makes cell size roughly coincident in with the area of field plots operationally established
150 and measured by Finnish Forest Centre (SMK, Suomen Metsäkeskus).

151 2.2. Field dataset used for validation

152 Field data for validation of the methods were partly acquired by University of Eastern Finland
153 (UEF), partly provided by SMK. A total of $N = 244$ plots were acquired in a stratified random
154 sampling fashion with approximately equal per-stratum sample sizes (Valbuena et al., 2016b).
155 The strata employed were the forest development classes commonly used in operational
156 management in Finland (per-stratum sample sizes were $n = 31$, unless specified): *Seedling*,
157 *Sapling*, *Young*, *Advanced*, *Mature*, *Shelterwood*, *Seed-tree* ($n = 29$), and *Multi-storied* ($n =$
158 29). SMK's stand register data based on previous inventories was employed for the initial
159 randomization of field plot locations. Valbuena et al. (2016b) provides details about acquisition
160 protocol and processing of field data. Appendix B details the criteria used to assign a
161 development class to for each field plot, a task carried out independently by experienced SMK
162 personnel.

163 3. Methods

164 3.1. The rule-based method for stratifying forests based on ALS data

165 We used a deductive approach to thresholding using the L-moment ratios. The rules were
166 deduced from their mathematical properties, as opposed to using inductive, supervised, data-
167 driven optimization or classification:

- 168 • The value $Lcv = 0.5$ was used because it represents maximum entropy of tree sizes
169 (Valbuena et al. 2012); also recall that $Lcv = GC$ (see Appendix A.3). Since Lcv
170 describes the relative dispersion of ALS heights, we postulated that Lcv could be used
171 as descriptor for structural properties related to tree size inequality, and hypothesised
172 that this threshold could be suitable for discriminating forests with trees of
173 approximately equal sizes – even tree sizes – ($Lcv < 0.5$) from those with high tree size
174 inequality – uneven tree sizes – ($Lcv > 0.5$).
- 175 • The value of $Lskew = 0$ was chosen because it represents a symmetric distribution of
176 ALS heights, and distinguishes plots with positive or negative skewness (Hosking,
177 1989). Being a descriptor of asymmetry, we postulated that $Lskew$ could be used as
178 descriptor for structural properties related to competitive dominance and light
179 availability characteristics (Valbuena et al., 2013a), and hypothesised that this threshold
180 could be useful for discriminating oligophotic zones ($Lskew < 0$) from euphotic ones
181 ($Lskew > 0$).

182 We classified forests throughout the scanned area according to these rules directly, avoiding
183 the use of field data in the training stage of the classification. The capacity of these rules to
184 describe structural features of the forest was validated by comparing the classifications at field
185 plot locations to the known development classes determined at the field plots. For that purpose,
186 the development classes were aggregated into the target forest structural properties:
187 even/uneven tree sizes and oligophotic/euphotic.

188 3.2. Aggregation of development classes

189 With the intention to study the hypothesised relationship between these thresholds of L-
190 moment ratios for ALS height distribution and their related structural properties of forests, we
191 aggregated the forest development classes according to their structural properties. In even-aged
192 silviculture, the succession of development classes usually follows this a basic chronosequence
193 of even-sized forest types: *Seedling*, *Sapling*, *Young*, *Advanced* and *Mature* stands. Silviculture
194 based on natural regeneration yields more complex uneven-sized structural types: *Shelterwood*,
195 *Seed-tree*, and *Multi-storied* stands. In Finland, *Shelterwood* stands are forest areas attaining
196 regeneration of shade-tolerant species under the shade casted by a closed dominant *Mature*
197 canopy (Appendix B). This is the oligophotic zone (Lefsky et al., 2002), which in the context
198 of Eurasian Boreal forests corresponds to regeneration areas for Norway spruce (note: there are
199 many different types of shelterwood management systems and, although in Finland this term
200 is used specifically for shade-tolerant regeneration – Appendix B –, in other countries it may
201 refer to regeneration of shade-intolerant species too, e.g. Valbuena et al., 2013a). Other
202 oligophotic areas are those which have reached the stem exclusion stage – *Young*, *Advanced*
203 and *Mature* stands –, limiting light availability under the dominant canopy (Zenner, 2005). On
204 the other hand, *Seed-tree* stands are areas where few parent trees provide seeds for natural
205 regeneration which recruits in the understory generating *Multi-storied* stands (Appendix B).
206 These, as well as *Seedling* and *Sapling* stands, belong to the euphotic zone (Lefsky et al., 2002),
207 where the absence of a closed dominant canopy brings enough light to the ground as to allow
208 the growth of shade-intolerant species. Accordingly, to test the capacity of the $Lcv = 0.5$ and
209 $Lskew = 0$ rules to discriminate forest areas according to their respective hypotheses, the
210 development classes were aggregated as:

211 (1) First criterion. Inequality among tree sizes ($Lcv = 0.5$):

- 212 • Even tree size forest structural types: *Seedling*, *Sapling*, *Young*, *Advanced* and *Mature*
213 stands. Characterized by low relative dispersion in tree sizes (Valbuena et al., 2013a).
- 214 • Uneven tree size forest structural types: *Shelterwood*, *Seed-tree* and *Multi-storied*
215 stands. Characterized by high relative dispersion in tree sizes (Valbuena et al., 2013a).
- 216 (2) Second criterion. Relative dominance of overstorey over the understorey ($Lskew = 0$):
- 217 • Oligophotic (forest structural types with a closed dominant canopy not allowing shade-
218 intolerant regeneration): *Young*, *Advanced*, *Mature* and *Shelterwood* stands.
219 Characterized by negative asymmetries (Valbuena et al., 2013a).
- 220 • Euphotic (forest structural types with canopy openness allowing shade-intolerant
221 regeneration): *Seedling*, *Sapling*, *Seed-tree*, and *Multi-storied* stands. Characterized by
222 positive asymmetries (Valbuena et al., 2013a).

223 3.3. Comparison against supervised classification

224 In order to compare the rule-based method with more common data-driven methodologies
225 based on inductive statistical inference, we contrasted the results against those obtained by a
226 supervised classification. For that purpose, we employed the results obtained in Valbuena et
227 al. (2016b) from a support vector machine (SVM) classification which employed the same field
228 plot dataset at the training stage as the one used for accuracy assessment in the present study.
229 SVM is becoming increasingly popular for classification of ALS data (Dalponte et al., 2008;
230 García et al., 2011), since it is suitable for operating with big datasets and complex relationships
231 of covariance. SVM is a hard classifier which calculates hyperplanes between classes under a
232 cost function defined as a combination of maximizing distances from training samples to the
233 hyperplanes while minimizing the error of misclassified samples. Using package *e1071* in R
234 statistical environment (Meyer et al., 2014a) and a SVM C-classification method, Valbuena et

235 al. (2016b) computed predictions of all the above-mentioned development classes separately
236 which, in the present study, we aggregated into the established criteria: inequality (even and
237 uneven tree size classes) and dominance (oligophotic and euphotic), as detailed above. It may
238 be worth noting that, in contrast to the rule-based method which avoided the training stage, the
239 SMV predictions were obtained by an error minimization method using field data support and
240 the explanatory capacity of many more ALS metrics (Valbuena et al., 2016b: Table 2).

241 3.4. Accuracy assessment.

242 Field data plots were only used for assessing the accuracy of the rule-based method.
243 Relationships among L-moments of ALS heights were observed in scatterplots which depicted
244 the development class to which each plot belonged, observing the role of different development
245 classes in these relationships. Development classes were grouped as described above, and the
246 capacity of the $Lcv = 0.5$ and $Lskew = 0$ rules to describe those grouping characteristics was
247 assessed with the help of contingency matrices. The degree of misclassification was evaluated
248 by the final overall accuracy (OA) and per-class user's (UA) and producer's (PA) accuracies,
249 which were all calculated following Olofsson et al.'s (2013) estimators for stratified random
250 sampling as:

$$251 \quad (3) \quad OA = \sum p_{ii} ;$$

$$252 \quad (4) \quad UA = \frac{p_{ii}}{p_{i.}} ;$$

$$253 \quad (5) \quad PA = \frac{p_{jj}}{p_{.j}} ,$$

254 calculated from the proportions of the total area for each predicted (i) and observed (j) class.
255 Given the stratified random sampling design, and to adjust the accuracy estimates to account
256 for the unequal sampling intensities for each class, these proportions were weighted according

257 to the share of area for each class (A_j) with respect to the total (A_t) (Olofsson et al., 2013), as
258 observed from the SMK's stand register dataset employed in the initial stratified random
259 sampling (Appendix B):

260 (6)
$$p_{ij} = \frac{A_j n_{ij}}{A_t N},$$

261 where n_{ij} was the number of plots observed for class j and predicted to be class i , and N the
262 total number of plots. Similarly, Cohen's (1960) kappa coefficient (κ) was also calculated from
263 these weighted proportions p_{ij} , employing the sample estimator for stratified random sampling
264 suggested by Stehman (1996). Routines implemented in R-packages *vcd* (Meyer et al., 2014b)
265 and *diffeR* (Pontius & Santacruz, 2015) were employed for these tasks. Results were compared
266 with those resulting from grouping supervised SVM predictions, which were obtained in a
267 leave-one-out fashion (Valbuena et al., 2016b). It is worth stating that the study design
268 complied with Westfall et al.'s (2011) recommendations for stratified estimation.

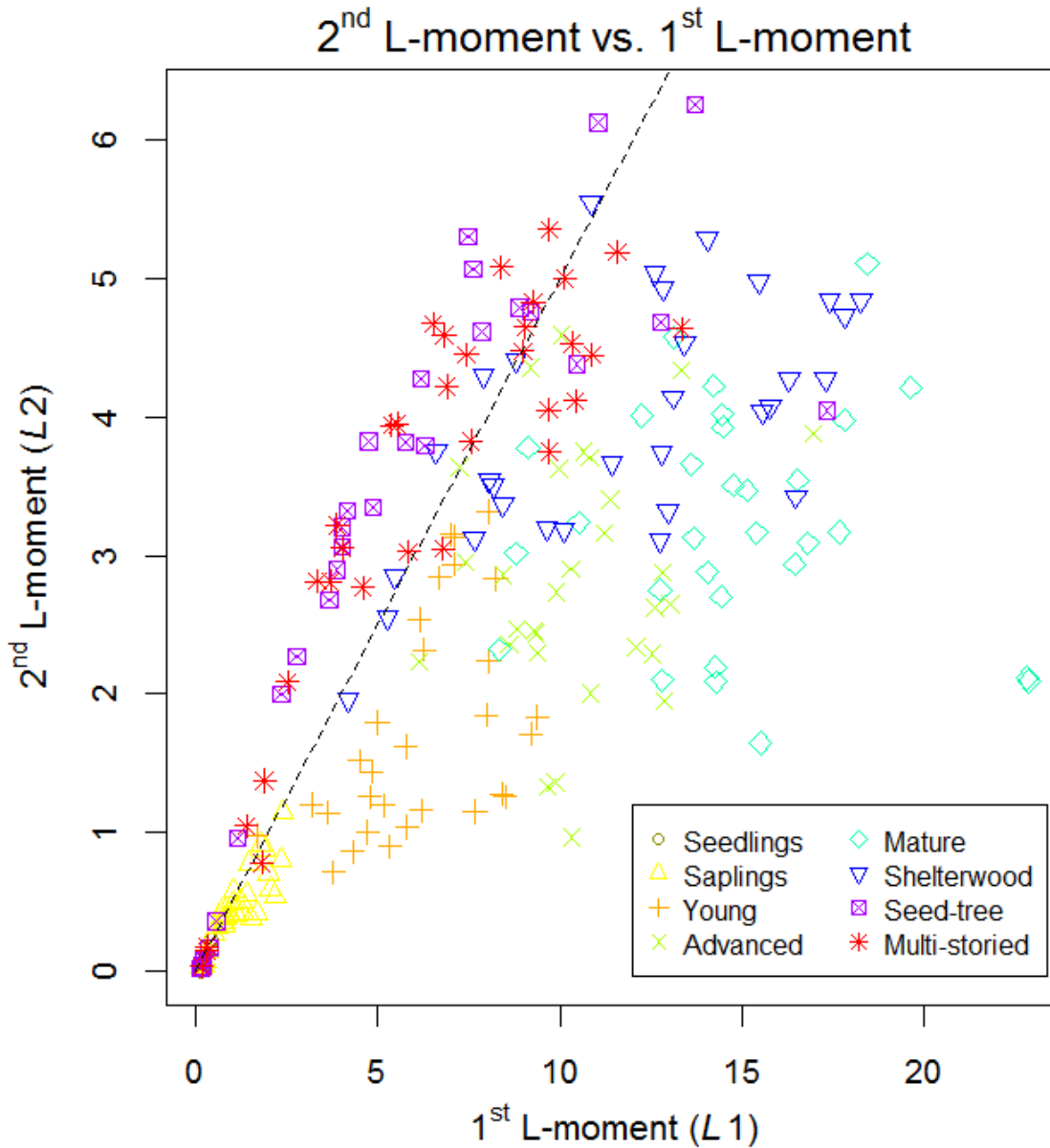
269 **4. Results**

270 *4.1. L-coefficient of variation of ALS heights*

271 First, we studied the relation between the *Lcv* of ALS heights and the forest development
272 classes observed at field plots. From Eq. (1), the rule $Lcv = 1/2$ can be represented in the $L2 \sim$
273 $L1$ relation (dashed line in Fig. 1) as:

274 (7)
$$L2 = \frac{L1}{2}.$$

275



276

277 **Figure 1.** Relationship between the first and the second L-moments of ALS heights (i.e., L-
 278 coefficient of variation).

279

280 The $Lcv = 0.5$ threshold in Eq. (7) is depicted in Fig. 1 with a dashed line. Thus, Fig. 1 shows
 281 how the different forest development classes distribute themselves at either side of this
 282 threshold, using ALS metrics only. We observed that *Seed-tree* and *Multi-storied* stands, which
 283 usually present large values of relative dispersion in tree sizes ($GC > 0.5$), also had wide

284 dispersion in their ALS returns being mainly above the threshold at $Lcv > 0.5$ as well. This
285 rule, however, failed to identify forest areas with regeneration of shade-tolerant species
286 recruited in the understorey under a closed dominant canopy. These correspond mainly to the
287 *Shelterwood* development class, which fell largely under $Lcv < 0.5$. Fig. 1 shows that
288 *Shelterwood* areas were difficult to discriminate from *Mature* forests, and hence they were
289 likely to be misclassified by this rule as being even tree size forest types. Fig. 1 also shows the
290 lack of independence of $L2$ from $L1$, since the spread of $L2$ values is larger for increasing $L1$.
291 This demonstrates the advantage of the Lcv ratio, which normalizes the values of dispersion in
292 $L2$, making them comparable among distributions differing in the mean ALS height ($L1$, see
293 Eq. A3 in Appendix A).

294 Concerning the classification results, using the $Lcv = 0.5$ rule for discriminating even tree size
295 (*Seedling*, *Sapling*, *Young*, *Advanced* and *Mature*) versus uneven tree size classes
296 (*Shelterwood*, *Seed-tree* and *Multi-storied*) (Table 1), obtained an overall accuracy of 92.4%
297 and a coefficient of agreement $\kappa = 0.48$. A total of 92.7% of the even-sized plots were correctly
298 classified by this rule, with only few omission/commission errors. Most uncertainty was on the
299 identification of uneven tree size forests, due to the inability for the $Lcv = 0.5$ rule to identify
300 *Shelterwood* areas (Fig. 1), as this rule only classified 24.4% of those areas as being uneven-
301 sized.

302

303

304

305

306 **Table 1.** Direct rule $Lcv = 0.5$. Contingency matrix of classification of even-sized versus
 307 uneven-sized development classes.

Predicted	Observed		Totals
	even-sized	uneven-sized	
even-sized	139	48	187
uneven-sized	11	46	57
Totals	150	94	244

308

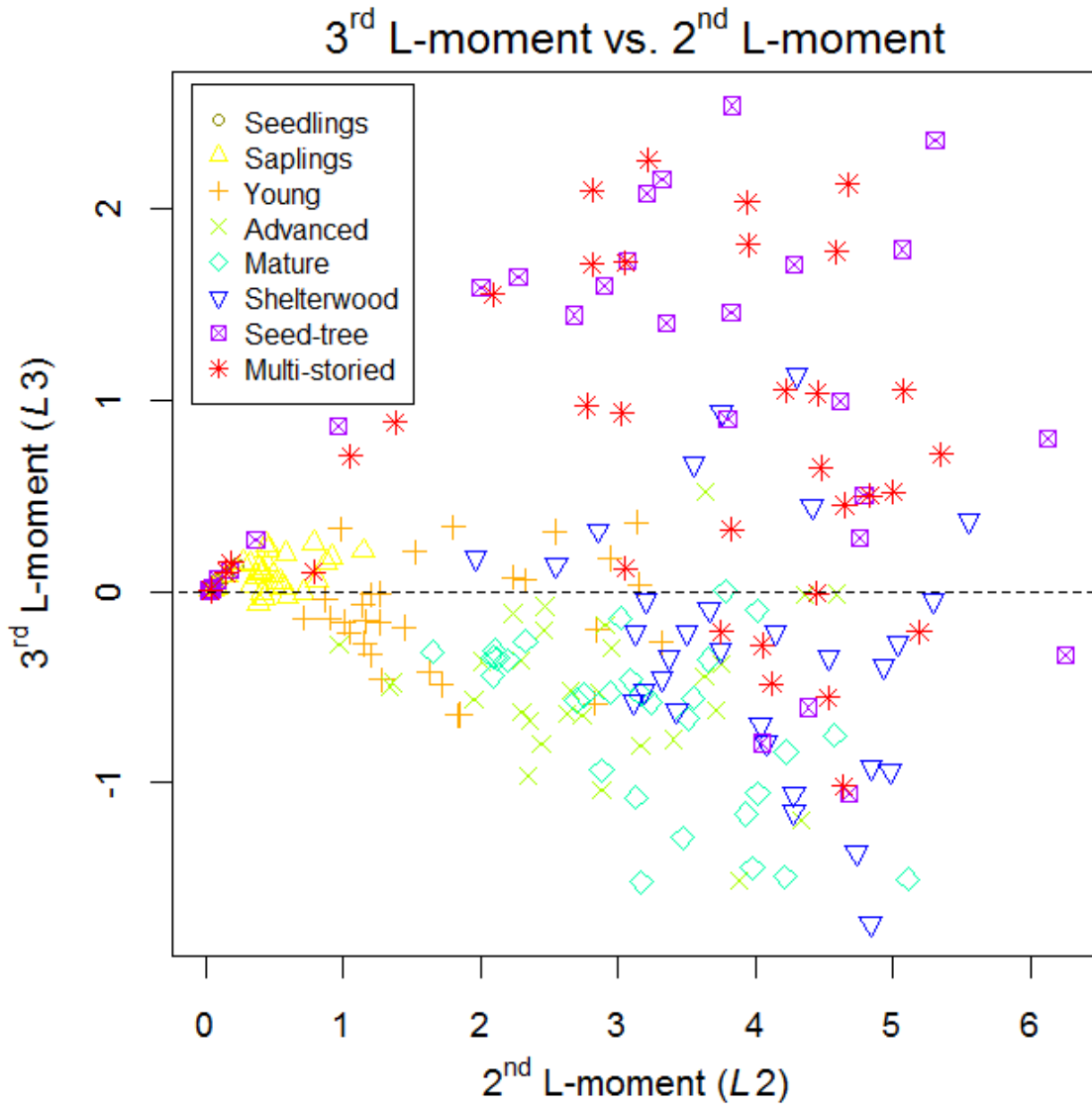
309 *4.2. L-skewness of ALS heights*

310 The next step was to observe the capacity of *Lskew* to incorporate additional information about
 311 forest structure with regards to the relationships of relative dominance among the trees. Using
 312 the rule $Lskew = 0$ in Eq. (2) gives

313 (8) $L3=0.$

314 Therefore the rule is demonstrated directly by the zero value on the y-axis of the $L3 \sim L2$
 315 relation (horizontal dashed line in Fig. 2). In Fig. 2, we also observed a strong dependency of
 316 $L3$ on $L2$, since the spread of $L3$ values expands while $L2$ increases. This also illustrates the
 317 advantages of the *Lskew* ratio, which normalizes the $L3$ values of asymmetry, making them
 318 comparable among distributions of differing dispersion of ALS heights (hence, of different
 319 mean ALS height as well).

320



321

322 **Figure 2.** Relationship between the second and third L-moments of ALS heights (i.e., L-
 323 skewness).

324

325 The utility of analysing the asymmetry of the ALS height distributions was clear, as *Lskew*
 326 was associated with the capacity of penetration of the laser pulses, and therefore with the
 327 openness of the canopy. Positive skewness ($Lskew > 0$) was observed when there were large
 328 proportions of ALS returns with relatively lower heights, which indicates few dominant trees
 329 allow the laser beam to reach lower areas underneath an open upper canopy. On the other hand,

330 negative skewness ($Lskew < 0$) was observed when a closed dominant canopy backscatters
 331 most returns from the higher strata, and only few of them are returned from the understorey.
 332 Regarding the discrimination of oligophotic (*Young, Advanced Mature and Shelterwood,*) and
 333 euphotic (*Seedling, Sapling, Seed-tree and Multi-storied*) areas of the forest (Table 2), the
 334 overall accuracy obtained was 84.6% and $\kappa = 0.56$. These accuracies were quite large,
 335 considering a method making no use of field data, an indication that *Lskew* may be a good
 336 proxy for the degree of canopy closure.

337

338 **Table 2.** Direct rule $Lskew = 0$. Contingency matrix of classification of oligophotic (closed
 339 canopies) versus euphotic (open canopies) areas.

		Observed		
Predicted		oligophotic	Euphotic	Totals
oligophotic		102	17	119
euphotic		19	106	125
Totals		121	123	244

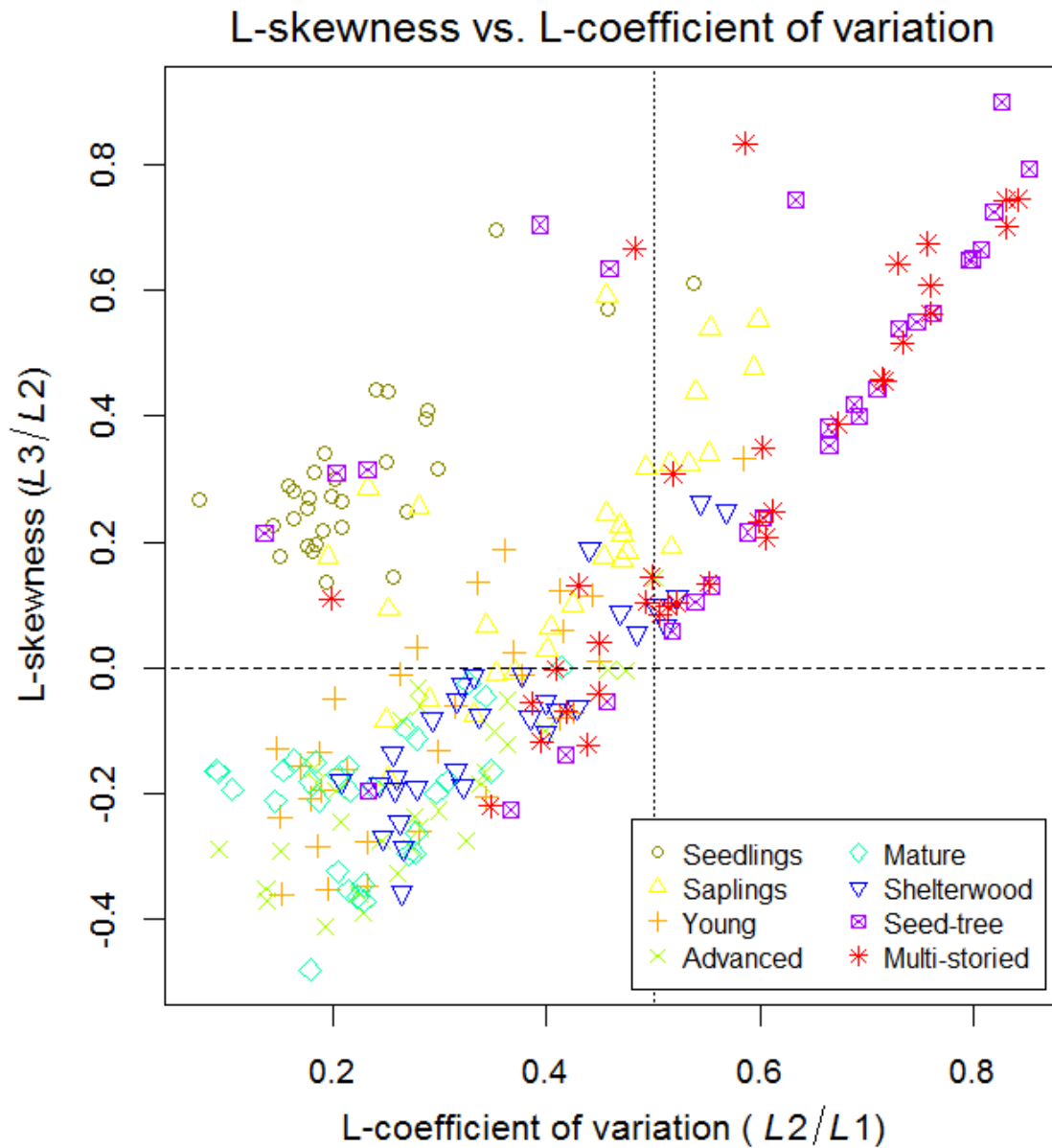
340

341 4.3. Comparing rule-based versus supervised method

342 Figure 3 shows a joint representation of both rules: $Lcv = 0.5$ and $Lskew = 0$, respectively
 343 represented by vertical dotted and horizontal dashed lines. It therefore illustrates how these
 344 measures of relative dispersion and asymmetry may be selected or combined in pursue of
 345 different objectives for classifying forest structure and development directly from the
 346 distribution of ALS returns. Furthermore, we also compared all results with those obtained by
 347 a supervised classification carried out with this same subsample dataset. Tables 3 and 4 are

348 contingency matrices for the aggregation of development classes (according to section 3.2)
349 predicted by the supervised SVM classification. For direct comparison, Table 5 includes a
350 summary of results obtained by all the compared methods.

351



352

353 **Figure 3.** Relationship between the L-coefficient of variation and L-skewness of ALS heights.

354

355 **Table 3.** Supervised classification. Aggregated classes from Valbuena et al. (2016b).
 356 Contingency matrix of classification of even-sized versus uneven-sized development classes.

		Observed		
Predicted	even-sized	uneven-sized	Totals	
even-sized	131	15	146	
uneven-sized	19	79	98	
Totals	150	94	244	

357

358 **Table 4.** Supervised classification. Aggregated classes from Valbuena et al. (2016b).
 359 Contingency matrix of classification of oligophotic (closed canopies) versus euphotic (open
 360 canopies) areas.

		Observed		
Predicted	oligophotic	Euphotic	Totals	
oligophotic	114	10	124	
euphotic	7	113	120	
Totals	121	123	244	

361

362

363

364

365

366

367 **Table 5.** Comparison of accuracy results.

Stratification	Rule-based classification	Supervised classification*
Even vs. Uneven Tree Size	<i>Lcv</i> = 0.5	SVM
Overall accuracy (<i>OA</i>)	92.4%	87.3%
kappa (κ)	0.48	0.34
Even tree size omission (<i>PA</i>)	92.7%	87.3%
Even tree size commission (<i>UA</i>)	99.6%	99.8%
Uneven tree size omission (<i>PA</i>)	48.9%	84.0%
Uneven tree size commission (<i>UA</i>)	4.2%	4.1%
Oligophotic vs. Euphotic	<i>Lskew</i> = 0	SVM
Overall accuracy (<i>OA</i>)	84.6%	93.8%
kappa (κ)	0.56	0.80
Oligophotic omission (<i>PA</i>)	84.3%	94.2%
Oligophotic commission (<i>UA</i>)	96.8%	98.3%
Euphotic omission (<i>PA</i>)	86.2%	91.9%
Euphotic commission (<i>UA</i>)	52.9%	76.8%

368 *aggregated from Valbuena et al. (2016b).

369

370 Regarding the results obtained from the supervised classification, it can be observed that the
 371 classification of forest areas into even and uneven tree sizes (Table 3) reached an overall
 372 accuracy 87.3% and $\kappa = 0.34$, whereas oligophotic versus euphotic (Table 4) obtained overall
 373 accuracy of 93.8% and $\kappa = 0.80$. Differences between the rule-based method and the supervised
 374 approach were not so large if taking into account the simplicity and lack of involvement of

375 field data in the former one. User's accuracies obtained by the SVM classification were very
376 similar to those yielded by the rule-based method (Table 5), which demonstrates that they are
377 mainly due to differences in the proportions of area that each development class has from the
378 population, and not differences between the two methods. The success of the $Lcv = 0.5$
379 threshold in classifying the even and uneven tree size forests and $Lskew = 0$ for segregating
380 the oligophotic and euphotic areas of forest was remarkably good if compared to the supervised
381 classification, which did not obtain much greater accuracies. The comparison of user's and
382 producer's accuracies against the supervised classification however highlighted the two major
383 differences: the rule-based method increased the errors due to omission of uneven-sized areas
384 and commission of euphotic areas (Table 5).

385 **5. Discussion**

386 *5.1. L-coefficient of variation may identify tree size inequality*



387 Our prior presumption was that forests with trees of approximately equal sizes – i.e., even tree
388 size classes –, since they would backscatter most ALS returns from a single canopy stratum,
389 could be directly detected by low values of the Lcv of their ALS heights. Our results
390 corroborate this presumption, since 92.7% of the even tree size plots were correctly classified
391 by this rule (blue colour in Fig. 4 examples). Fig. 3 shows that most uncertainty in even tree
392 size areas – those containing trees of approximately equal sizes – was due to *Sapling* stands,
393 whereas not one single plot belonging to either *Advanced* or *Mature* development classes
394 showed values of $Lcv > 0.5$. The low rate of omission errors implies that this rule could be
395 used as a rather conservative and simple method when the purpose is to predict even tree size
396 forest areas.

397



Canopy Height Model

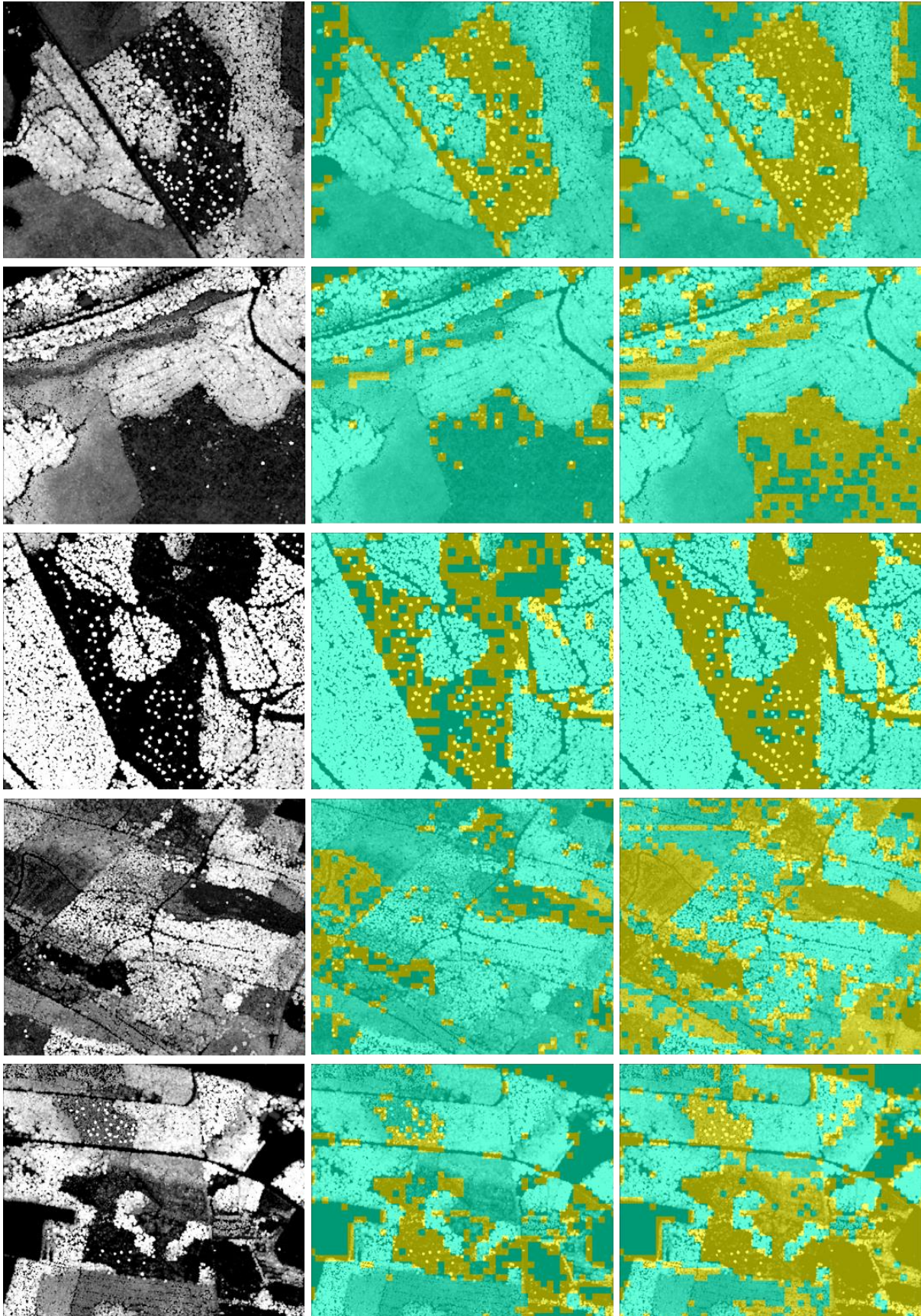
40 m  0 m

L-coefficient of variation

 < 0.5  > 0.5

L-skewness

 < 0  > 0



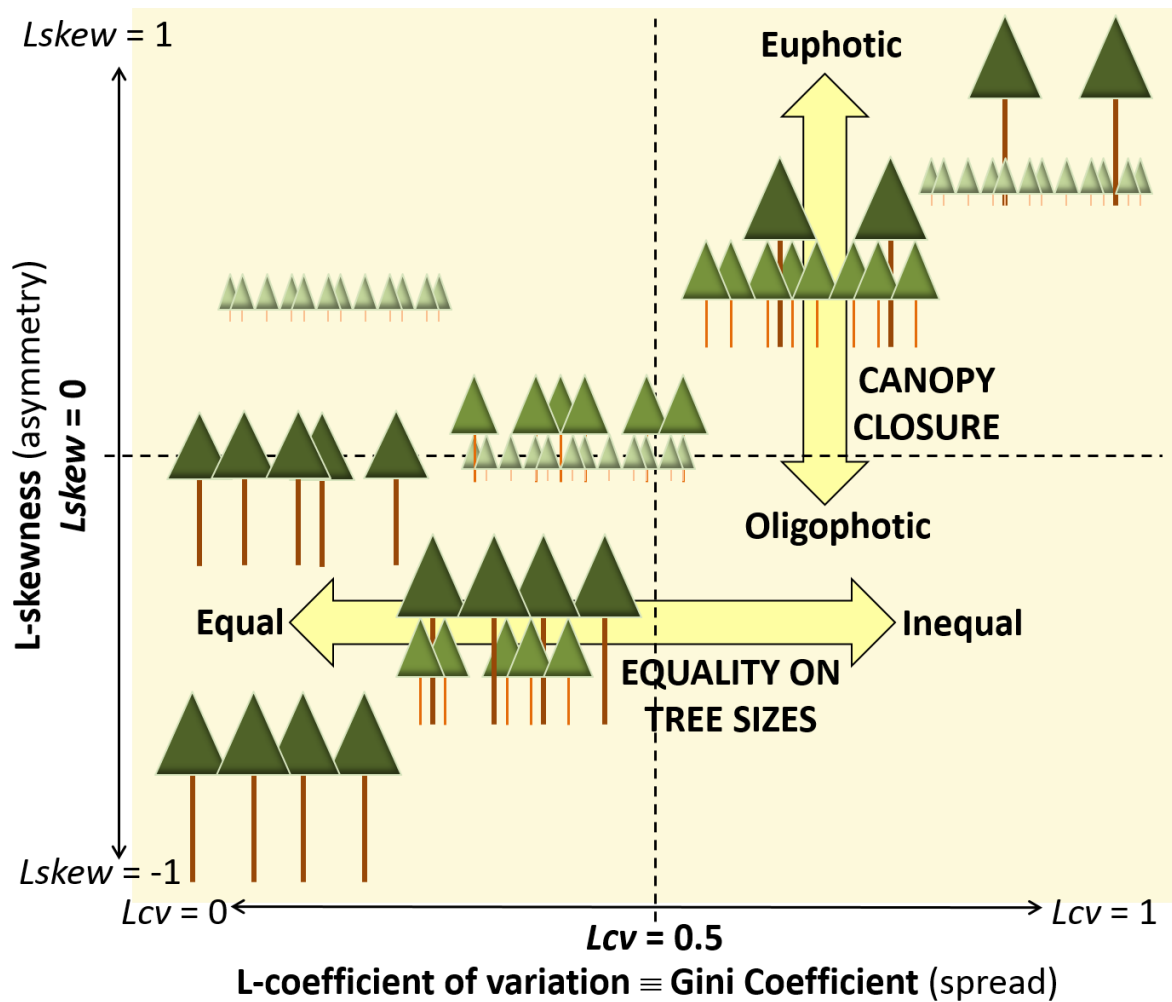
399 **Figure 4.** Examples of resulting maps of forests stratified with rule-based method. Left: canopy
400 height model (CHM). Middle: areas with $Lcv > 0.5$ in yellow (uneven tree sizes) and $Lcv <$
401 0.5 in blue (even tree sizes). Right: areas with $Lskew > 0$ in yellow (euphotic) and $Lskew <$
402 0 in blue (oligophotic). The reference CHM was made from the same ALS dataset, courtesy of
403 Aki Suvanto (Blom Kartta Oy).

404

405 On the other hand, it was also expected that in the presence of structurally heterogeneous forests
406 with more inequality of sizes among its trees, the ALS returns would also show a more spread
407 pattern as they backscatter along the full vertical profile of the canopy, showing higher values
408 of Lcv . In view of our results, that was the case for *Seed-tree* and most *Multi-storied* areas,
409 although not for *Shelterwood* stands. We therefore propose that the direct rule $Lcv > 0.5$ may
410 be used as an indicator of great tree size inequality only when regeneration is achieved by
411 shade-intolerant species, and therefore it has been enabled by forest disturbance (Knox et al.,
412 1989; Kellner & Asner, 2009). In other words, a correspondence between the GC of tree sizes
413 (Valbuena et al. 2013a) and the Lcv of ALS heights may only happen when the large value of
414 GC is due to the presence of a gap in the canopy, which allows a large proportion of the laser
415 footprint to get through and disperse its corresponding returns along the vertical profile of the
416 canopy (Stark et al., 2012). This highlighted the importance of employing an additional metric
417 discriminating areas with a large euphotic zone from those where regeneration occurs in the
418 oligophotic zone (Lefsky et al., 2002; Fig. 5). Whether or not more ALS metrics are required
419 for fully describing the structural properties of forests, it is worth noting the recurrence of Lcv
420 as a variable selected by many different automated methods tested in our previous studies, and
421 therefore the role of Lcv in predicting structural attributes related to tree size inequality

422 (Valbuena et al., 2013b; 2014; 2016a) and forest development (Valbuena et al., 2013a; 2016b)
 423 seems clear.

424



425

426 **Figure 5.** Schematic diagram representing the patterns of ALS return distribution that can be
 427 found in different types of forest structures, and how they are described by ratios of L-moments:
 428 L-coefficient of variation and L-skewness. Compare to Fig. 3 and Valbuena et al. (2013a: Fig.
 429 4).

430

431 Exploring the reasons why only 24.4% of *Shelterwood* stands were classified by the $Lcv > 0.5$
432 rule as being uneven-sized, it could be taken into account that this development class was also
433 the one showing most error in the SVM classification (Valbuena et al., 2016b). The fact that a
434 supervised method, which used the explanatory potential of many other metrics as well, still
435 failed to reliably identify *Shelterwood* areas may be an indication that the limitation is due not
436 to the metrics but rather to the original ALS data. Due to the low-density nature of this national
437 dataset (NLS, 2013), the laser footprint probably detects very infrequently the presence of
438 understory under closed dominant canopies. In that case, scan density would need to be
439 increased for this task. We considered the advantages of testing the rule-based method with
440 this type of ALS dataset since, due to its simplicity, could have potential for replication at
441 national scales. Further research should, however, employ datasets of larger densities to clarify
442 whether Lcv could then show better capacity for detecting regeneration of shade-tolerant
443 species. If direct replication of the rule-based method is to be envisaged, the effect of other
444 flight parameters in these L-moment ratios, such as scanner device or maximum scanning angle
445 (Næsset, 2004; Disney et al., 2010), should also be object of future investigations.

446 5.2. *L-skewness may identify fully closed canopies*

447 The threshold derived from the asymmetry measure of L-moments, $Lskew = 0$, was
448 demonstrably practical with regards to discriminating oligophotic from euphotic areas.
449 $Lskew < 0$ denotes areas where most ALS returns were backscattered from a closed dominant
450 canopy which only allows small proportions of the laser footprint – and the light resource – to
451 reach the understorey. Conversely, $Lskew > 0$ was observed whenever there were large
452 proportions of ALS heights with relatively lower heights, and it was therefore related to the
453 presence of only few returns backscattered from upper areas in the canopy, which indicates
454 that the dominant trees allow the laser beam – and thereby the light resource – to reach lower

455 areas underneath an open canopy. This can be relevant with regards to findings by Drake et al.
456 (2002) and Lefsky et al. (2005), who found the degree of canopy closure to be one of the most
457 relevant covariates in the relation between biomass and ALS heights.

458 It may be worth noting that the $Lskew > 0$ rule was capable for practically delineating
459 *Seedling*, *Sampling* and *Seed-tree* stands directly (Fig. 4). Although the method was carried out
460 at pixel-level, the resulting maps identified entire stands sharply. The rule-based stratification
461 by $Lskew > 0$ was therefore fairly insensitive to the within-stand variation that usually makes
462 difficult to discriminate stands, especially *Seed-tree* areas, by standard area-based procedures
463 in remote sensing. These type of problems usually require more complex analyses at object-
464 level – representing stands –, which involve segmentation procedures with subjective steps,
465 parameters determined by trial-and-error, or manual delineation (e.g., Pascual et al., 2008). In
466 contrast, the rule based method offers a simple procedure to determine *Seedling*, *Sampling* and
467 *Seed-tree* stands directly.

468 5.3. Synergies between the rules

469 Overall accuracies obtained by the rule-based methods were, respectively, 92.4% and 84.6%
470 which we considered a remarkable achievement for a rule-based method not requiring field
471 support for training and that they were comparable to the results obtained by the supervised
472 classification (87.3% and 93.8%, respectively; Table 5). As a rule of thumb, it may be affirmed
473 that $Lskew > 0$ characterizes canopies not fully closed (areas not having reached stem
474 exclusion), whereas those areas which also had values of $Lcv > 0.5$ presented high inequality
475 among tree sizes driven by forest disturbance (Fig. 5). In our results in Fig. 3, values of wide
476 dispersion $Lcv > 0.5$ occurred only in the presence of positive skewness $Lskew > 0$. This was
477 also corroborated out of the sample, as pixels with $Lcv > 0.5$ also had $Lskew > 0$ as well (Fig.
478 4). This demonstrates that, in these low-density datasets, the variance of ALS heights only

479 increases as a cause of openness in the canopy and an increase of the euphotic zone (Lefsky et
480 al., 2002), possibly due to forest disturbance, which leads to positive skewness in the
481 distribution. As a consequence, the maps obtained with $Lcv > 0.5$ were expanded by the
482 $Lskew > 0$ rule (Fig. 4), extending the areas of large tree size inequality towards those simply
483 presenting potential for growth with no limitation from light resource. In turn, negatively
484 skewed $Lskew < 0$ ALS height distributions (Fig. 2) are indicative of forests with large
485 oligophotic zone (Lefsky et al., 2002) and therefore can only allow the regeneration of shade-
486 tolerant species. It is worth commenting that uneven tree size and euphotic forest areas stand
487 out of a general relationship between first moments of ALS heights and forest attributes related
488 to mean diameter (Lefsky et al., 2002, 2005), and therefore we suggest that one potential use
489 of the rule-based method could to decrease the signal-to-noise ratio when obtaining ALS-
490 assisted estimations in heterogeneous forest areas.

491 *5.4. Practical benefits and further research needs*

492 In this article, we applied deductive science (Appendix A) to infer that L-moments from the
493 distribution of ALS returns can have a direct relationship to forest structural characteristics at
494 the community level, namely tree size inequality and canopy closure (Fig. 5), in addition to the
495 already well-known fact that ALS height relates to tree height (e.g., Lefsky et al., 2005;
496 Maltamo et al., 2005; Miura & Jones, 2010). The main benefit of these research findings is on
497 increasing our understanding (Fig. 5) of how ALS explains key structural features related to
498 forest structure (Gove, 2004; Valbuena et al., 2012) and tree competition (Weiner, 1990;
499 Cordonnier & Kunstler, 2015). These can be relevant to enhance the potential of ALS for
500 describing light availability conditions (Lefsky et al., 2002), forest disturbance characteristics
501 (Kellner & Asner, 2009), or tree growth (Stark et al., 2010) and regeneration (Valbuena et al.,
502 2013a). Further research should clarify the role of different flight configurations, scanners

503 systems or scanning density (Næsset, 2004; Disney et al., 2010) in the relationships between
504 ALS L-moments and forest structural characteristics.

505 The resulting classification could be used e.g. in stratification of a forest area for the field data
506 collection of an ALS inventory campaign, since Hawbaker et al. (2009), Maltamo et al. (2011)
507 and Gobakken et al. (2013) demonstrated that a field sampling strategy based on *a priori*
508 knowledge extracted from the ALS itself may be advantageous. In the presence of within-stand
509 heterogeneity (e.g., Valbuena et al., 2013a), L-moments could be valuable for delineating
510 microstands (van Aardt et al., 2006). There are potential applications in guiding future forest
511 management operations directly from ALS datasets, once unveiling the relationship between
512 *GC* and silvicultural alternatives (Pukkala et al., 2016) and thereby to L-moments of ALS
513 returns. For ecosystem studies, there is potential for studying canopy structure, e.g.,
514 discrimination of single- and multi-layered forests, and other traits relevant to old-growth
515 forests (Lefsky et al., 2002; Miura & Jones, 2010). We encourage further research to exploit
516 the potential of L-moments in forest estimation and other applications.

517

518 **6. Conclusions**

519 We developed a rule-based classification deduced from L-moments summarizing the relative
520 dispersion and skewness of ALS heights. Classification by two simple deductive mathematical
521 rules, L-coefficient of variation $Lcv > 0.5$ and L-skewness $Lskew > 0$, was carried out
522 directly on the ALS return cloud, omitting training stages making use of field plot data. Lcv
523 was related to tree size inequality, while $Lskew$ provided information on the degree of closure
524 of the dominant canopy. These provide relevant information about competition conditions in
525 different areas of the forest, which can be deduced directly from ALS datasets. Our
526 conclusions, however, may apply only to Boreal ecosystems, where light availability and its

527 interception by the dominant canopy is the competitive process that limits forest growth. Some
528 of the accuracies obtained were remarkably large, being a direct classification using no field
529 data support, and they were comparable to those obtained by a supervised classification. Two
530 flaws of the rule-based method were the omission of uneven-sized forest with shade-tolerant
531 regeneration and commission errors for the euphotic areas, to be solved by further research
532 perhaps making use of datasets with higher density. These rules can be executed directly over
533 ALS datasets, providing an unambiguous procedure with multiple applications.

534 **Acknowledgements**

535 This research was funded by Suomen Metsäkeskus (SMK Finnish Forest centre). Special
536 thanks to Juho Heikkilä and Jussi Lappalainen (SMK), Heli Laaksonen (NLS), and Aki
537 Suvanto (Blom Kartta Oy) for their support at different stages of this study. Rubén Valbuena
538 would like to thank The Finish Society of Forest Sciences for awarding a IUFRO Grant which
539 sponsored his travel to present this work at Silvilaser 2015 Conference in La Grande Motte
540 (France). Special issue editors are thanked for inviting this communication and three
541 anonymous reviewers for their helpful and constructive comments.

542 **References.**

- 543 Asner, G.P., & Mascaro J. (2014). Mapping tropical forest carbon: Calibrating plot estimates
544 to a simple LiDAR metric. *Remote Sensing of Environment*, 140, 614-624
- 545 Bollandsås, O.M., & Næsset, E. (2007). Estimating percentile-based diameter distributions in
546 uneven-sized Norway spruce stands using airborne laser scanner data. *Scandinavian Journal*
547 *of Forest Research*, 22, 33–47.
- 548 Cohen, J. (1960). A coefficient of agreement for nominal scales. *Educational and*
549 *Psychological Measurement*, 20 (1): 37–46

550 Cordonnier, T., & Kunstler, G. (2015). The Gini index brings asymmetric competition to
551 light. *Perspectives in Plant Ecology, Evolution and Systematics*, 17 (2), 107-115.

552 Dalponte, M. Bruzzone, L., Gianelle, D. 2008. Fusion of hyperspectral and LIDAR remote
553 sensing data for classification of complex forest areas. *IEEE Transactions in Geosciences
554 and Remote Sensing*, 46 (5), 1416-1427.

555 David, H.A., & Nagaraja, H.N. (2003). *Order Statistics* (third edition). Wiley Series in
556 Probability and Statistics. New York: John Wiley.

557 Disney, M.I., Kalogerou, V., Lewis, P., Prieto-Blanco, A., Hancock, S., & Pfeifer, M. (2010).
558 Simulating the impact of discrete-return lidar system and survey characteristics over young
559 conifer and broadleaf forests. *Remote Sensing of Environment*, 114, 1546-1560

560 Drake, J.B., Dubayah, R.O., Knox, R.G., Clark, D.B., & Blair, J.B. (2002) Sensitivity of large-
561 footprint lidar to canopy structure and biomass in a neotropical rainforest, *Remote Sensing of
562 Environment*, 81 (2-3), 378-392.

563 Frazer, G.W., Wulder, M.A., & Niemann, K.O. (2005). Simulation and quantification of the
564 fine-scale spatial pattern and heterogeneity of forest canopy structure: A lacunarity-based
565 method designed for analysis of continuous canopy heights, *Forest Ecology and Management*,
566 214 (1-3), 65-90.

567 Frazer G.W., Magnussen S., Wulder M.A., & Niemann K.O. (2011). Simulated impact of
568 sample plot size and co-registration error on the accuracy and uncertainty of LiDAR-derived
569 estimates of forest stand biomass. *Remote Sensing of Environment*, 115, 636-649.

570 García, M., Riaño, D., Chuvieco, E., Salas, J., Danson, F.M. 2011. Multispectral and LIDAR
571 Data Fusion for Fuel Type Mapping Using Support Vector Machine and Decision Rules.
572 *Remote Sensing of Environment*, 115 (6), 1369-1379.

573 Gini, C. (1921) Measurement of inequality of incomes. *Economic Journal*, 31, 124–26.

574 Gobakken, T., Korhonen, L. & Næsset, E. (2013). Laser-assisted selection of field plots for
575 an area-based forest inventory. *Silva Fennica*, 47 (5), 943.

576 Gove, J.H. (2004) Structural stocking guides: a new look at an old friend. *Canadian Journal*
577 *of Forest Research*, 34,1044–1056.

578 Hall, S. A., Burke, I. C., Box, D. O., Kaufmann, M. R. & Stoker, J. M. (2005). Estimating
579 stand structure using discrete-return lidar: An example from low density, fire prone
580 ponderosa pine forests. *Forest Ecology and Management*, 208 (1-3), 189-209.

581 Hawbaker, T.J., Keuler, N.S., Lesak, A.A., Gobakken, T., Contrucci, K., & Radeloff, V.C.
582 (2009). Improved estimates of forest vegetation structure and biomass with a LiDAR-
583 optimized sampling design. *Journal of Geophysical Research*, 114, G00E04.

584 Helmert, F.R. (1876) Die Berechnung des wahrscheinlichen Beobachtungsfehlers aus den
585 ersten Potenzen der Differenzen gleichgenauer director Beobachtungen. *Astronomische*
586 *Nachrichten*, 88, 127–132.

587 Hosking, J.R.M. (1989). Some theoretical results concerning L-Moments. *Research Report*
588 *RC14492*. IBM research, Yorktown Heights.

589 Hosking, J.R.M. (1990). L-Moments: Analysis and Estimation of Distributions Using Linear
590 Combinations of Order Statistics. *Journal of the Royal Statistical Society. Series B*
591 *(Methodological)*, 52, 105–124.

592 Jaskierniak, D., Lane, P.N.J., Robinson, A., & Lucieer, A. (2011). Extracting LiDAR indices
593 to characterise multilayered forest structure using mixture distribution functions. *Remote*
594 *Sensing of Environment*, 115, 573-585

595 Kellner, J.R. & Asner, G.P. (2009) Convergent structural responses of tropical forests to
596 diverse disturbance regimes. *Ecology Letters*, 12, 887–897

597 Kleiber, C. (2005) The Lorenz curve in economics and econometrics. Invited paper, Gini-
598 Lorenz Centennial Conference, Siena (Italy).

599 Knox, R.G., Peet, R.K. and Christensen, N.L. 1989. Population dynamics in loblolly pine
600 stands: Changes in skewness and size inequality. *Ecology*, 70, 1153-1167

601 Lefsky, M. A., Cohen, W. B., Acker, S. A., Spies, T. A., Parker, G. G., & Harding, D.
602 (1999a). Lidar remote sensing of biophysical properties and canopy structure of forest of
603 Douglas-fir and western hemlock. *Remote Sensing of Environment*, 70, 339– 361.

604 Lefsky, M.A., Harding, D., Cohen, W.B., Parker, G., & Shugart, H.H. (1999b). Surface Lidar
605 Remote Sensing of Basal Area and Biomass in Deciduous Forests of Eastern Maryland, USA.
606 *Remote Sensing of Environment*, 67, 83-98.

607 Lefsky, M.A., Cohen, W.B., Parker, G., & Harding, D., (2002). Lidar remote sensing for
608 ecosystem studies. *Bioscience*, 52, 19-30.

609 Lefsky, M.A., Hudak, A.T., Cohen, W.B., and Acker, S.A. (2005). Patterns of covariance
610 between forest stand and canopy structure in the Pacific Northwest. *Remote Sensing of*
611 *Environment*, 95, 517-531

612 Maltamo, M., Packalen, P., Yu, X., Eerikainen, K., Hyypä, J., & Pitkanen, J. (2005).
613 Identifying and quantifying structural characteristics of heterogeneous boreal forests using
614 laser scanner data. *Forest Ecology and Management*, 216, 41–50.

615 Maltamo, M., Bollandås, O.M., Næsset, E., Gobakken, T., & Packalén, P. (2011). Different
616 plot selection strategies for field training data in ALS-assisted forest inventory. *Forestry*, *84*,
617 23-31

618 Miura, N. & Jones, S.D. (2010). Characterizing forest ecological structure using pulse types
619 and heights of airborne laser scanning, *Remote Sensing of Environment*, *114* (5), 1069-1076.

620 Meyer, D., Dimitriadou, E., Hornik, K., Weingessel, A. & Leisch, F. (2014a) e1071: Misc
621 Functions of the Department of Statistics, TU Wien. R package version 1.6-4.
622 <http://ugrad.stat.ubc.ca/R/library/e1071/html/00Index.html>. Visited in Jan. 2014.

623 Meyer, D., Zeileis, A. and Hornik, K. (2014b) vcd: Visualizing Categorical Data. R package
624 version 1.3-2. <https://cran.r-project.org/web/packages/vcd/index.html> Visited in Jan. 2014.

625 NLS - National Land Survey of Finland 2013. Laser scanning data (available online at
626 maanmittauslaitos.fi). Visited in Sep. 2013.

627 Næsset, E. (2002). Predicting forest stand characteristics with airborne scanning laser using a
628 practical two-stage procedure and field data. *Remote Sensing of Environment*, *80*, 88-99.

629 Næsset, E. (2004). Effects of different flying altitudes on biophysical stand properties
630 estimated from canopy height and density measured with a small-footprint airborne scanning
631 laser. *Remote Sensing of Environment*, *91* (2), 243-255.

632 Ozdemir, I., & Donoghue, D.N.M. (2013). Modelling tree size diversity from airborne laser
633 scanning using canopy height models with image texture measures. *Forest Ecology and*
634 *Management*, *295*, 28–37.

635 Pascual, C., García-Abril, A., García-Montero, L.G., Martín-Fernández, S., & Cohen, W.B.
636 (2008) Object-based semi-automatic approach for forest structure characterization using lidar

637 data in heterogeneous *Pinus sylvestris* stands. *Forest Ecology and Management*, 255 (11),
638 3677-3685.

639 Pontius, R.G., & Santacruz, A. (2015). diffeR: Metrics of Difference for Comparing Pairs of
640 Maps. R package version 0.0-4. <http://CRAN.R-project.org/package=diffeR>. Visited in Apr.
641 2016.

642 Pukkala, T., Laiho, O., & Lähde, E. (2016). Continuous cover management reduces wind
643 damage. *Forest Ecology and Management*, 372, 120-127

644 Robbins, H.E. (1944). On the Expected Values of Two Statistics. *The Annals of Mathematical*
645 *Statistics*, 15, 321-323.

646 Stark, S.C., Leitold, V., Wu, J.L., Hunter, M.O., de Castilho, C.V., Costa, F.R., McMahon,
647 S.M., Parker, G.G., Shimabukuro, M.T., Lefsky, M.A., Keller, M., Alves, L.F., Schiatti, J.,
648 Shimabukuro, Y.E., Brandão, D.O., Woodcock, T.K., Higuchi, N., de Camargo, P.B., de
649 Oliveira, R.C., Saleska, S.R., & Chave, J. (2012). Amazon forest carbon dynamics predicted
650 by profiles of canopy leaf area and light environment. *Ecology Letters*, 15 (12), 1406-1414.

651 Olofsson, P., Foody, G.M., Stehman, S.V., & Woodcock, C.E. (2013) Making better use of
652 accuracy data in land change studies: Estimating accuracy and area and quantifying uncertainty
653 using stratified estimation, *Remote Sensing of Environment*, 129, 122–131.

654 Stehman, S.V. (1996) Estimating the Kappa coefficient and its variance under stratified random
655 sampling. *Photogrammetric Engineering & Remote Sensing*, 62 (4), 401–402.

656 Valbuena, R., Packalen, P., Martín-Fernández, S., & Maltamo, M. (2012). Diversity and
657 equitability ordering profiles applied to study forest structure. *Forest Ecology and*
658 *Management*, 276, 185–195.

659 Valbuena, R., Packalen, P., Mehtätalo, L., García-Abril, A., & Maltamo, M. (2013a).
660 Characterizing forest structural types and shelterwood dynamics from Lorenz-based
661 indicators predicted by airborne laser scanning. *Canadian Journal of Forest Research*, *43*,
662 1063–1074.

663 Valbuena, R., Maltamo, M., Martín-Fernández, S., Packalen, P., Pascual, C., & Nabuurs, G.J.
664 (2013b). Patterns of covariance between airborne laser scanning metrics and Lorenz curve
665 descriptors of tree size inequality. *Canadian Journal of Remote Sensing*, *39*, S18–S31.

666 Valbuena, R., Vauhkonen, J., Packalen, P., Pitkänen, J., Maltamo, M. (2014) Comparison of
667 airborne laser scanning methods for estimating forest structure indicators based on Lorenz
668 curves. *ISPRS Journal of Photogrammetry & Remote Sensing*, *95*, 23–33

669 Valbuena, R., Eerikäinen, K., Packalen, P. & Maltamo, M. (2016a). Gini coefficient
670 predictions from airborne lidar remote sensing display the effect of management intensity on
671 forest structure. *Ecological Indicators*, *60*, 574–585.

672 Valbuena, R., Maltamo, M. & Packalen, P. (2016b). Classification of multi-layered forest
673 development classes from low-density national airborne lidar datasets. *Forestry*, *89*, 392–401.

674 van Aardt, J.A.N., R.H. Wynne, & Oderwald, R.G. (2006). Forest volume and biomass
675 estimation using small-footprint LiDAR-distributional parameters on a per-segment basis.
676 *Forest Science*, *52* (6), 636-649.

677 Wang, Q. J. (1996). Direct sample estimators of L moments. *Water Resources Research*, *32*
678 (12), 3617–3619.

679 Weiner, J. (1990) Asymmetric competition in plant populations. *Trends in Ecology and*
680 *Evolution*, *5*, 360–364.

681 Westfall, J. A., Patterson, P. L., & Coulston, J. W. (2011). Post-stratified estimation: within-
682 strata and total sample size recommendations. *Canadian Journal of Forest Research*, 41 (5),
683 1130–1139.

684 White, J.C.; Wulder, M.A.; Varhola, A.; Vastaranta, M.; Coops, N.C.; Cook, B.D.; Pitt, D.;
685 Woods, M. (2013). *A best practices guide for generating forest inventory attributes from*
686 *airborne laser scanning data using an area-based approach*. Natural Resources Canada,
687 Information Report FI-X-010. Canadian Forest Service, Victoria, BC.

688 Zenner, E.K. (2005). Development of tree size distributions in Douglas-fir forests under
689 differing disturbance regimes. *Ecological Applications*, 15, 701-714

690 Zimble, D.A., Evans, D.L., Carlson, G.C., Parker, R.C., Grado, S.C., & Gerard, P.D. (2003).
691 Characterizing vertical forest structure using small-footprint airborne LiDAR. *Remote Sensing*
692 *of Environment*, 87, 171-182.

693 **Appendix A. L-moments and their relationship to Gini Coefficient**

694 *A.1. L-moments for describing a distribution*

695 Let an order statistic $X_{k:r}$ be the k -th smallest observation in a sample of size r of the random
696 variable X (e.g. ALS return heights), and let $E(X_{k:r})$ be its expected value. For example,
697 consider $E(X_{1:2})$ in the following population of size 3: {12,16,14}. There are three possible
698 samples of size $r = 2$, with sample minima ($k = 1$): {12,12,14}. The expected value is the
699 mean over these, i.e., $E(X_{1:2}) = 12.67$. In the analysis of this paper, the population is the
700 unknown infinite set of all possible ALS returns over the primary calculation unit (sample plot
701 or grid cell). The expected value is estimated using the observed sample of returns.

702 L-moments describe the distribution of a scalar random variable X through weighted sums of
 703 $E(X_{k:r})$. Hosking (1990) defined the L-moments as:

$$704 \quad (A1) \quad Lr = r^{-1} \sum_{k=0}^{r-1} (-1)^k \cdot \binom{r-1}{k} \cdot E(X_{r-k:r}).$$

705 The first L-moment ($L1$) is obtained by substituting $r = 1$ in equation (A1) to get:

$$706 \quad (A2) \quad L1 = E(X_{1:1}) = E(X),$$

707 which is thus equivalent to the first product-moment (expectation) of X . Hence, $L1$ is the L-
 708 measure for the location or central tendency of the distribution. If observations of X are
 709 available, $L1$ can be estimated as the arithmetic mean:

$$710 \quad (A3) \quad \widehat{L1} = \bar{X}.$$

711 The second L-moment ($L2$), follows the case for $r = 2$:

$$712 \quad (A4) \quad L2 = \frac{1}{2} E(X_{2:2}) - \frac{1}{2} E(X_{1:2}) = \frac{1}{2} E[X_{2:2} - X_{1:2}],$$

713 which is the expected value of half difference between minimum ($X_{1:2}$) and maximum ($X_{2:2}$)
 714 in a sample of size two. It therefore provides the mean of half differences, and thus it is the L-
 715 measure for the dispersion of the distribution.

716 Following a similar logic for the third L-moment ($L3$), substituting $r = 3$ in (A1) yields:

$$717 \quad (A5) \quad L3 = \frac{1}{3} E(X_{3:3}) - \frac{2}{3} E(X_{2:3}) + \frac{1}{3} E(X_{1:3}),$$

718 which is a weighted sum of minimum, ($X_{1:3}$), median ($X_{2:3}$), and maximum ($X_{3:3}$) of a sample
 719 with size three. It can further be written as:

$$720 \quad (A6) \quad L3 = \frac{1}{3} E[(X_{3:3} - X_{2:3}) - (X_{2:3} - X_{1:3})],$$

721 to show that $L3$ expresses the expected difference between the maximum-median and median-
 722 minimum differences in a sample of size three, which provides a L-measure for the asymmetry
 723 of the distribution of X . Hence, $L3 = 0$ corresponds to a symmetric distribution, $L3 > 0$
 724 describes positive asymmetry (left-skewed distribution) and $L3 < 0$ describes negative
 725 asymmetry (right-skewed distribution).

726 *A.2. L-moment ratios*

727 Hosking (1990) also defined the ratios for L-moments. They have the advantage of being
 728 bounded by finite intervals (Hosking 1989), yielding comparable relative descriptions for the
 729 distribution of X .

730 The second L-moment ratio is obtained as the ratio of the second to the first L-moments. It is
 731 called the L-coefficient of variation (Lcv) for its comparison to conventional moments. From
 732 equations (A2) and (A4) it can be observed that Lcv equals:

733 (A7)
$$Lcv = \frac{L2}{L1} = \frac{E(X_{2:2}) - E(X_{1:2})}{2E(X)}.$$

734 For positive random variables, the values for the second L-moment ratio are bounded by the
 735 $[0, 1]$ range (Hosking, 1989). Just like the coefficient of variation of conventional moments,
 736 Lcv is a descriptor of dispersion relative to central tendency; that is to say, concentration. This
 737 brings the advantage that concentration measures are comparable among distributions differing
 738 in their location or central tendency ($L1$), and also independently of the units of measure. It is
 739 worthwhile to note that Hosking never defined a second L-moment ratio, as their generalized
 740 definition stands only for $r = 3, 4 \dots$ (Hosking 1990: 108), and the L-coefficient of variation
 741 was simply presented alongside. It was only later that many authors have regarded Lcv to be
 742 the second L-moment ratio.

743 The third L-moment ratio is obtained by division between the third and the second L-moments.
 744 It is called the L-skewness (*Lskew*), as it has been found to be a robust descriptor for the
 745 asymmetry of the distribution of X . From equations (A4) and (A6), and using the equivalence
 746 $E(X_{3:3} - X_{1:3}) = \frac{3}{2}E(X_{2:2} - X_{1:2})$ (Robbins, 1944: Eq. 22; David & Nagaraja, 2003: 44, 56) it
 747 yields:

$$748 \quad (A8) \quad Lskew = \frac{L3}{L2} = \frac{E(X_{3:3}) - 2E(X_{2:3}) + E(X_{1:3})}{E(X_{3:3}) - E(X_{1:3})}.$$

749 As explained for $L3$, $Lskew = 0$ corresponds to a symmetric distribution, while positive or
 750 negative values denote the type of asymmetry for the distribution. Additionally, $Lskew$ has the
 751 advantage of presenting theoretical bounds within the $[-1, 1]$ interval (Hosking 1989).
 752 Consequently, $Lskew$ is a descriptor of asymmetry relative to dispersion, and therefore
 753 independent of the units of measure and the dispersion of the distribution of X .

754 *A.3. Equivalence between the Gini coefficient and the L-coefficient of variation*

755 The Gini coefficient of a scalar random variable X (GC) is the ratio of the area comprised
 756 between the Lorenz curve and the diagonal line of equality (Gini, 1921):

$$757 \quad (A9) \quad GC = 1 - 2 \int_0^1 L(X) dX,$$

758 Where $L(X)$ is the Lorenz curve: the relative cumulative distribution of a variable against the
 759 cumulative frequency distribution of the proportion of individuals in the population. From Eq.
 760 (A9), Kleiber (2005: Eq. 6) showed that:

$$761 \quad (A10) \quad GC = 1 - \frac{E(X_{1:2})}{E(X)}.$$

762 On the other hand, the Lcv gives also the GC . From Eq. (A7) it derives:

$$\begin{aligned}
763 \quad (A11a) \quad Lcv &= \frac{E(X_{2:2}) - E(X_{1:2})}{2E(X)} \\
764 \quad (A11b) \quad &= \frac{E(X_{2:2} - X_{1:2}) + 2E(X_{1:2}) - 2E(X_{1:2})}{2E(X)} \\
765 \quad (A11c) \quad &= \frac{E(X_{2:2} + X_{1:2}) - 2E(X_{1:2})}{2E(X)} \\
766 \quad (A11d) \quad &= \frac{2E(X) - 2E(X_{1:2})}{2E(X)} \\
767 \quad (A11e) \quad &= 1 - \frac{E(X_{1:2})}{E(X)}
\end{aligned}$$

768 Equation (A11d) results from (A11c) because $X_{1:2} + X_{2:2}$ is the sum of two independent and
769 identically distributed samples, and it is therefore equivalent to $X_1 + X_2$. Consequently, (A10)
770 and (A11e) demonstrate:

$$771 \quad (A12) \quad GC = Lcv$$

772 The result in Eq. (A12) is essentially a special case of a 140-years-old result (Helmert, 1876;
773 as cited in David and Nagaraja, 2003: 249) presented in equation 9.4.2 of David and Nagaraja
774 (2003), which might even provide interesting extensions using expectations of order statistics
775 in sample sizes larger than $r = 1, 2, 3$.

776

777 **Appendix B. Criteria for determining forest development classes**

778 Silvicultural development classes are used in Finland to classify forest stands and assist in
779 decision-making for forest management planning. It was possible to apply stratified sampling
780 using the stand register dataset employed by the Finnish Forest Centre (SMK, Suomen
781 Metsäkeskus) for their operational management planning, since a development class has been

782 explicitly assigned to each stand from previous inventories. The development class to which
783 each sample plot belonged to was nevertheless ultimately corroborated in the field, being the
784 criteria used *in-situ* prevalent over the stand register data. Minor differences in per-stratum
785 sample sizes were simply caused by such type of discrepancies found in few plots. The criteria
786 that segregated forest areas into different forest classes were:

- 787 • *Seedling*: stands with average tree height lower than 1.3 m, and absence of mature trees
788 (overstorey).
- 789 • *Sapling*: stands with average tree height greater than 1.3 m, and average diameter at
790 breast height (DBH) smaller than 8 cm, and absence of mature trees (overstorey).
- 791 • *Young*: stands with average DBH ranging 8-16 cm and average tree height ranging 7-9
792 m high.
- 793 • *Advanced*: stands with average DBH greater than 16 cm.
- 794 • *Mature*: stands reaching a quadratic mean DBH (QMD) greater than 18 cm.
- 795 • *Shelterwood*: stands including a dense overstorey of mature trees (DBH > 16 cm) which
796 reaches at least 100-300 stems·ha⁻¹, and also a dense understorey of seedlings (height <
797 1.3 m) of shade-tolerant species, usually Norway spruce (1500-1800 stems·ha⁻¹).
- 798 • *Seed-tree*: stands including a sparse overstorey of mature trees (DBH > 16 cm) of only
799 50-100 stems·ha⁻¹, and also a dense understorey of seedlings (height < 1.3 m) of shade-
800 intolerant species, usually Scots pine (1500-2200 stems·ha⁻¹) or Birch species (1100-
801 1600 stems·ha⁻¹).
- 802 • *Multi-storied*: stands including a dense understorey (above-mentioned densities) of
803 seedlings (height < 1.3 m) and saplings (height > 1.3 m, DBH < 8 cm) of any species,
804 usually deciduous but also Scots pine or Norway spruce. The size of trees in the
805 overstorey is not a determinant criterion, but trees in the understory must reach their
806 sapling stage.